Strong Pyramidal Growth of Metal Films Studied with IR Transmittance and Surface Enhanced IR Absorption of CO

A. Priebe,* G. Fahsold, and A. Pucci†

Kirchhoff-Institut für Physik, Ruprecht-Karls-Universität, Im Neuenheimer Feld 227, D-69120 Heidelberg, Germany

Received: July 5, 2004; In Final Form: September 20, 2004

Metal-film surfaces show well ordered facets if grown at sufficiently high temperature and at relatively small deposition rate. Such films may grow as pyramids that become increasingly steep with more coverage. On MgO(001) at about 400 °C iron forms nanoparticles with a shape like cuboids. These cuboids avoid coalesce with further deposition, and therefore they are an interesting system for effects that involve field enhancement, like for example surface enhanced infrared absorption of adsorbate vibrations. In this work we show that for such films the percolation is extended over a broad coverage range. Surface enhanced infrared absorption of CO adsorbed on the film shows the asymmetry of the C−O stretch line, which is typical for films near the percolation threshold. Both the line shape and the line intensity do not change remarkably above a certain average film thickness.

1. Introduction

Film growth is a nonequilibrium process, where kinetics plays an important role also at higher substrate temperatures. The kinetic processes that may lead to the formation of well ordered arrays of particles of the similar size and shape are the diffusion over potential barriers at step edges (Ehrlich−Schwoebel barrier),[1] the deflection of incoming atoms from the original atom-beam direction due to a highly corrugated surface, and shadowing for oblique incidence onto such a surface. Such particles are stabilized by the typically lower surface energy of oxide and halide surfaces compared to that of the metal. This is particularly true in the case of Fe on MgO, where the surface free energy of Fe is 2.9 J/m^2 [2] and of MgO is 1.1 J/m^2.[3]

In this work we consider nanostructured metal films of Fe on MgO(001) grown at 400 °C and at a deposition rate of about 0.15 nm/min. Metal films grown under such conditions of sufficiently high temperature and relatively small deposition rate have well ordered facets.[4] These films may grow as pyramids that become increasingly steep with increasing coverage.[5] On MgO(001) the iron forms rather cuboids than pyramids because of the high temperature.[6] The cuboids do not really coalesce with further deposition and, therefore, are an interesting system for studying surface enhanced infrared absorption (SEIRA).

Here we report on the infrared (IR) characterization of the free charge carriers in such films and of their coupling to the stretching vibration of adsorbed CO molecules. This coupling gives the so-called field enhancement, which we consider as the main contribution to SEIRA for that system.

2. Experimental Section

The in-situ experiments were performed with a vacuum Fourier transform IR spectrometer (Bruker IFS 66 v/S with midrange mercury−cadmium−telluride detector) attached to an ultrahigh vacuum (UHV) chamber (base pressure $<2 \times 10^{-8}$ Pa). In more detail, the experimental setup is described somewhere else; e.g., see ref 7. This setup allows infrared transmission spectroscopy during thin film growth under UHV conditions. Metal-film thicknesses are calculated from the deposition time and the rate (typically 0.15 nm/min assuming Fe bulk density), which was calibrated with a quartz microbalance. Substrate temperatures were measured by a chromel−alumel thermocouple attached to the sample holder. The MgO(001) substrates were prepared in UHV by cleavage of 7 × 7 × 15 mm^3 sized single crystals. After cleavage, the temperature was raised to 400 °C, and Fe was deposited at an average angle of incidence of 30°. Atomic force microscopy (AFM) pictures were immediately taken after the UHV experiments. For experimental details on the AFM experiments see ref 8. After Fe film preparation the samples were cooled to about 100 K and exposed to CO (purity 99.997 vol %, $p_{CO} = 2 \times 10^{-6}$ Pa). During exposure we measured the transmittance change of the sample with a spectral resolution of 2 cm^{-1}. A total of 50 scans per spectrum were sampled within 20 s. The IR transmittance spectra of this study were measured at normal incidence of light.

3. Results and Discussion

3.1. Iron Film. As published previously at room-temperature coalescence of iron films on MgO occurs between 0.7 and 1 nm average film thickness.[12] However, at 400 °C the iron islands on UHV cleaved MgO(001) grew as cuboids (see Figure 1), which seemed to avoid coalescence.[9−11] Even for an average thickness up to 32 nm these cuboids appear as clearly separated in AFM pictures. The top planes of the cuboids are looking evenly as a result of layer-by-layer growth that could be expected at this high temperature.[13,14] It is known that the large mobility of Fe adatoms on Fe islands allows the development of well-defined crystalline island facets at 400 °C.[13]

In Figure 2 experimental transmittance spectra of Fe on MgO-(001) at 400 °C are shown for a selection of average film thicknesses *d*. The slope of the spectra corresponds to a dynamic conductivity that increases with frequency up to an average

* Corresondig author. E-mail: apriebe@ix.urz.uni-heidelberg.de.
† E-mail: a.pucci@ix.urz.uni-heidelberg.de.

10.1021/jp047042k CCC: $27.50
Published on Web 11/03/2004

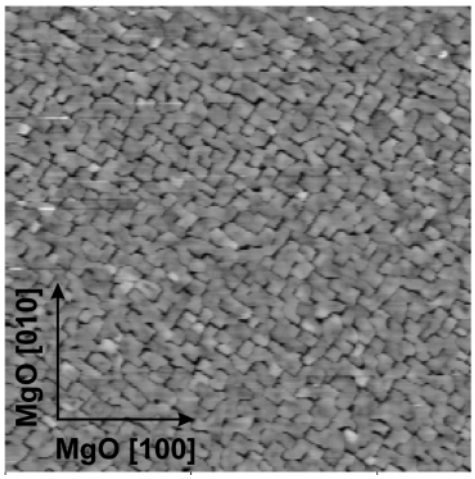

Figure 1. AFM image of 20 nm Fe grown at 400 °C. The MgO(001) substrate surface was prepared by cleavage in UHV. The scanned area is 5 μm × 5 μm. The orientation of the substrate is indicated.

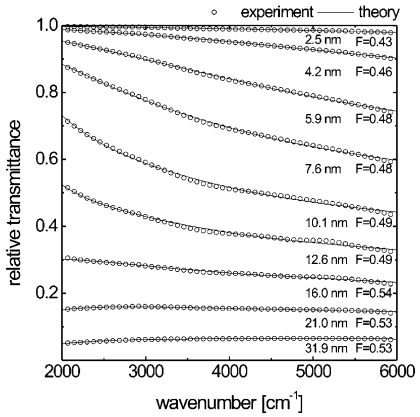

Figure 2. Selection of IR transmittance spectra (circles, only each tenth data point is shown) at normal incidence of Fe films grown at 400 °C (with respect to the MgO substrate transmittance). The substrate was prepared by cleavage in UHV. The average metal thickness as measured with a quartz microbalance is given in nanometers. The fitted curves (lines) well agree with the experimental data in the whole spectral range. The calculation is based on eq 1.

thickness of about 15 nm. Above this thickness we observed a nearly frequency independent relative transmittance that is only slowly decreasing with further metal deposition. A constant transmittance is known as an indicator of the percolation threshold.[15] Hence, it simply follows that films with thickness above 15 nm should stay in the vicinity of the percolation threshold. For comparison at 420 °C Jordan et al. found continuous 10 nm thick Fe films on MgO, but for higher temperature they observe islandlike films[10] like in our study. That difference certainly is due to the higher surface defect density of their MgO substrates, which had been prepared differently.[12] The AFM pictures from our films correspondingly show that film coalescence is inhibited. They show a dense packing of separated cuboids but the grooves occupy only a small fraction of the substrate surface; see Figure 1. Vice versa, the coverage of the substrate by metal particles is about 80% which is well above 50% that is the filling factor F for the percolation threshold of the two-dimensional Bruggeman model.[16] The filling $F = 50\%$ results from our fit calculations for 15 nm average thickness.

For the spectral calculations we used the effective dielectric function ϵ_{eff} according to the two-dimensional Bruggeman dielectric function with the relation.[16]

$$F\frac{\epsilon_{\mathrm{m}} - \epsilon_{\mathrm{eff}}}{\epsilon_{\mathrm{m}} + \epsilon_{\mathrm{eff}}} = (F-1)\frac{\epsilon - \epsilon_{\mathrm{eff}}}{\epsilon + \epsilon_{\mathrm{eff}}} \quad (1)$$

This model is known as a good approximation for metal films that consist of one layer of particles with similar shapes.[16] Particularly, in two dimensions that model is reasonable; it is valid also at the percolation threshold because the Bruggeman dielectric function becomes incorrect only in the fifth-order of perturbation theory.[17,18] In eq 1 the dielectric function of the material between the islands is ϵ, which is vacuum for pure metal films. The dielectric function of the metal is denoted by ϵ_{m} and is described on the basis of a Drude-type model

$$\epsilon_{\mathrm{m}}(\omega,d) = 1 - \frac{\omega_{\mathrm{p}}^{2}(\omega,d)}{\omega[\omega + \mathrm{i}\omega_{\tau}(\omega,d)]} \quad (2)$$

For the calculation of the spectra of iron films it is important to take account of the frequency dependence of the Drude parameters relaxation rate $\omega_{\tau}(\omega,d) = \omega_{\tau\mathrm{bulk}}(\omega) + \omega_{\tau\mathrm{surface}}(d)$ and plasma frequency $\omega_{\mathrm{p}}(\omega,\mathrm{d}) = \beta(d)\omega_{\mathrm{pbulk}}(\omega)$, where $\omega_{\tau\mathrm{surface}}(d)$ and $\beta(d)$ takes the surface effects into account.[19] The spectra of Figure 2 can be well fitted with that model. The fit parameters are F (fit results given in Figure 2), $\omega_{\tau\mathrm{surface}}(d)$ (e.g., $\omega_{\tau\mathrm{surface}}(d = 5.9\ \mathrm{nm}) \approx 2200\ \mathrm{cm}^{-1}$, $\omega_{\tau\mathrm{surface}}(d = 32\ \mathrm{nm}) \approx 1200\ \mathrm{cm}^{-1}$), and $\beta(d)$ (e.g.: $\beta(d = 5.9\ \mathrm{nm}) \approx 4.4$, $\beta(d = 32\ \mathrm{nm}) \approx 3$).[20] It has to be mentioned that $\omega_{\tau\mathrm{surface}}(d)$ and $\beta(d)$ mainly shift the transmittance curve whereas F mostly changes the slope of the transmittance spectrum for the shown thickness range. The best-fit parameters, like, for example, a filling factor close to 50% for films above 15 nm, need further comment: The best fits to the spectra within the two-dimensional Bruggeman model give a plasma frequency of the metal component significantly bigger than the bulk value (factor $\beta > 1$). That result means enhanced particle absorption, which is well-known in the literature.[21,22] But here we have to admit that the iron dielectric function, particularly the temperature dependence of the frequency dependent part is not known in the infrared region.[23] The exact quantitative analyses of iron spectra needs further studies, at first on the IR material properties at various temperatures. Nevertheless, the calculated parameters need an explanation. First they show that such calculation cannot give the true metal-particle properties particularly for a system with a statistics different to a random two-dimensional arrangement of dots. The result with a certain F and, for example, with $\beta = 3$ only says that a layer of metal dots covering the part F of the plane has the same transmittance spectrum like the respective real film consisting of iron cuboids if ω_{p} would be three times higher than in iron. The only reasonable result of such fit calculation is the finding that the films above 15 nm must be close to percolation because $F = 0.5$ is the filling factor for the percolation of the two-dimensional Bruggeman model. Because the cuboids array clearly has another statistics than a random occupation of lattice sites by spheres the Bruggeman fit cannot give the right numerical values for the material data of the iron islands.

3.2. IR Absorption Lines of CO on Iron Films. IR spectroscopy in normal transmission geometry is nonsensitive to CO adsorbed on a smooth metal surface, as the dipole moment is roughly perpendicular to the E-Feld it is not SEIRA active there.[8] Using the infrared transmission spectroscopy and a SEIRA active surface, one can easily detect the C−O stretch line of relatively small amounts of molecules. The dense metal-cuboids arrangement of the iron films prepared at 400 °C on MgO (001) offers sites with the field enhancement. CO exposed

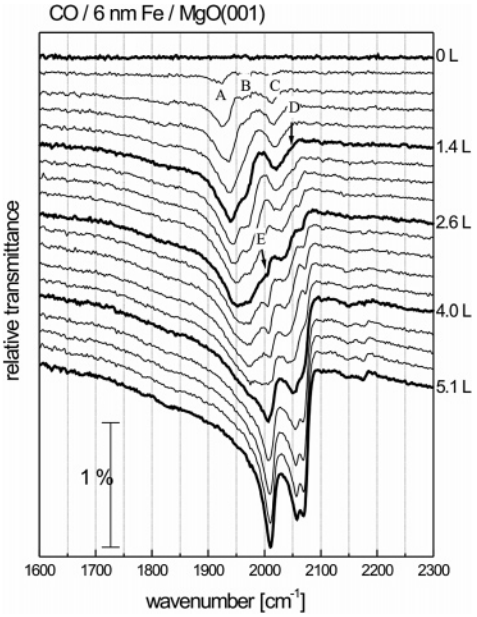

Figure 3. Development of normalized IR transmittance of normal incidence of 6 nm Fe on MgO(001) with increasing CO exposure (as labeled in Langmuir) at 100 K. The iron films were grown at 400 °C. For A, B, C, D, and E, see text.

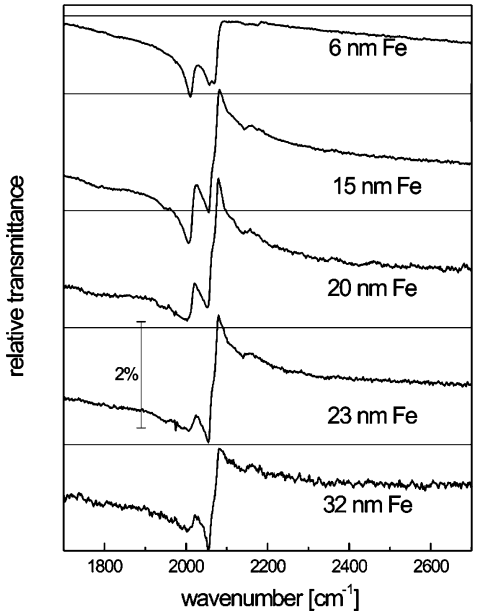

Figure 4. Normalized IR transmittance of normal incidence at the saturation exposure of CO on Fe films with average film thickness *d* as indicated. The saturation exposure was 5.1, 7.8, 8.8, 9.7, and 11.9 langmuir for increasing average film thickness. Reference spectrum: transmittance of the pure film at 100 K. The thin lines indicate 100%.

to these films at 100 K gives strong lines with asymmetric shape that we observed in the C−O stretching region. The spectra show different absorption features corresponding to three different CO adsorption sites, possibly on different facets. Figure 3 shows the exposure dependent absorption of the C−O stretching mode of CO adsorbed on a 6 nm thick Fe film.

For small coverage we find the absorption peaks at 1924 cm^{-1} (A) and at 1965 cm^{-1} (B) of CO known for 2-fold sites on the (011) and (001) facet.[24−26] Also we can see another adsorption feature (C) of CO corresponding to the on top position of the (001) facet[24] at 2010 cm^{-1} that shifts to 2059 cm^{-1} with increasing exposure. After an exposure of ∼1.4 langmuirs of CO we find an additional absorption feature (D) at 2055 cm^{-1} that shifts to 2073 cm^{-1}. Also, this can be assigned to the CO on the on top position of the (001) facet.[26] Interestingly, we find two adsorption peaks, whereas Moon et al.[26] found only one absorption feature at 2073 cm^{-1} for the on-top position of the (001) facet as well as Benndorf et al.,[24] who found only one at 2055 cm^{-1}. In our experiments IR reflectance at grazing incidence on smooth and continuous films annealed at high temperature we also saw only the absorption peak at the higher frequency.[8] The reason for the two different adsorption lines could be a reconstruction of the (001) facet[27] or tension, but this needs further studies. At about 2.4 langmuirs we observe the adsorption feature (E) of CO on top of the (011) facet at 2005 cm^{-1}. This peak shifts up to 2016 cm^{-1}.

The spectral changes due to CO adsorption at 100 K onto iron films of different thickness are shown in Figure 4 for exposures that correspond to saturation of the IR spectral features. For 23 nm average iron thickness saturation is about 10 L that is more than 3 times the saturation exposure for low-index Fe surfaces at about 100 K.[24] The saturation exposure further increases with film thickness. We found out an almost linear relationship between average film thickness and saturation exposure; see Figure 5. There is no important reason to assume different CO sticking coefficients at the various metal particle facets. Therefore, the observed saturation behavior must have another reason. This could be the reduction of the effective exposure to a metal particle sidewall due to its partial shading

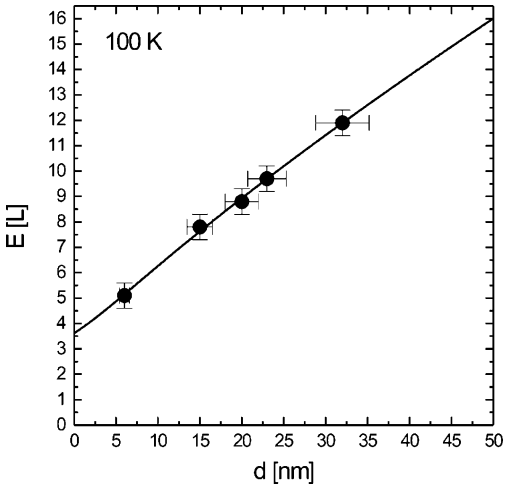

Figure 5. Saturation exposure *E* of CO for the different Fe thicknesses derived from the observed saturation of the IR spectral changes (closed circles). The line was calculated by eq 4 with $E_0 = 1.8$ langmuir and $w = 7$ nm.

by the neighbor particle. The effect is more important as the groves between the particles deepen. A simple calculation should demonstrate this idea: Assuming that the width *w* of the groves is small with respect to the length of the groves between the cuboids, we can estimate the reduction *f* of the steradian for striking molecules;

$$f(x) = \frac{\arctan\left(\frac{w}{x}\right)}{\pi} \tag{3}$$

which depends on the position *x* in the groves. Therefore, the saturation exposure *E* depending on the depth of the groves $d_g = d/F$ can be estimated as

$$E(d_g, w, E_0) = E_0 \frac{d_g}{\int_0^{d_g} f(x)\,dx} \tag{4}$$

where E_0 is the saturation exposure for the single-crystal surface. Here we have to admit that the observed saturation of the IR signal is more sensitive to the saturation for sites with the highest enhancement. Nevertheless, we get a good fit to the observed saturation coverage; see Figure 5. The fit parameters are $E_0 =$ 1.8 langmuir and $w = 7$ nm, which is a reasonable result. For example, for CO on Fe(001) $E_0 = 2.5$ langmuir is found.[20]

Also for the thicker films (Figure 4) we find both the structures (C) and (D) for the (001) facet. Due to the higher asymmetry the feature at 2073 cm^{-1} only appears as a shoulder in the spectra. From changes of the intensity ratio of the absorption lines (C) at 2059 cm^{-1} and (E) at 2016 cm^{-1}, respectively, for increasing average film thickness it follows that the size ratio between the different facets has changed. At higher thickness the line (C) at 2059 cm^{-1} dominates the spectrum. Because the line occurs in normal transmittance, the side faces of the Fe cuboids should have the (100) orientation, which is in accordance to the statement on the increase of steepness with thickness.

From Figure 4 it becomes obvious that the spectral background has changed due to adsorption. This is the so-called adsorbate induced baseline shift.[28] Near the percolation threshold the background polarizability of the adsorbate layer influences the broadband transmittance of a metal film additionally to the surface-friction effect from the adsorbates and to their charge transfer, which makes a straight quantitative evaluation impossible.[29,30]

The CO lines look unusual. Vibration lines in IR spectra may become broadened and asymmetric because of the dipole−dipole interaction between the differently adsorbed species.[31] But the dipole−dipole interaction cannot explain the peculiar asymmetry observed in this experiment. The pronounced transmittance increase above the baseline that occurs at frequencies close to the transmittance minimum on the high-frequency side is a typical SEIRA feature found near percolation.[30] In principle, it can be reproduced with effective media models if they are valid close to percolation, like for example, the two-dimensional Bruggeman model.[32] The other mechanism that may lead to Fano-type vibration lines is the electron−hole (eh) pair mechanism, where vibration excitations interact with eh excitations. This interaction may give additional enhancement in SEIRA and SERS for adsorbates on cold-condensed metal films, but it is not effective for metal facets formed at high temperatures.[33,34] For $d \geq 15$ nm the asymmetry is remarkably higher compared to the 6 nm thick film, for example. This finding is consistent with the one from above; i.e., the films hardly overcome the percolation threshold.[29,35]

The signal height (peak-to-peak height) of the asymmetric features in the C−O stretching region is of the order of 2%, which is surprisingly big for a transmittance experiment. That signal size points to SEIRA, and we want to estimate the enhancement factor with respect to the signal of the same spatial arrangement of CO without metal. Because the preparation of such samples is not possible in reality, we will estimate the enhancement in transmittance spectra on the basis of IR reflection−absorption spectra for CO on smooth iron films.[8] Because of that, we also need to know the metal-island area density and the CO covered area of the metal-island sidewalls. For the structures in the AFM image of 20 nm film (Figure 1) and from the deposited volume, the effective CO covered area of the sidewalls is about half the area of the plane surface. To get an estimate for the vibrational polarizability α_{CO} from the IR reflection−absorption, we use an approximation for the relative reflectance $\Delta R/R$ of p-polarized light at angle ϕ of incidence,[36]

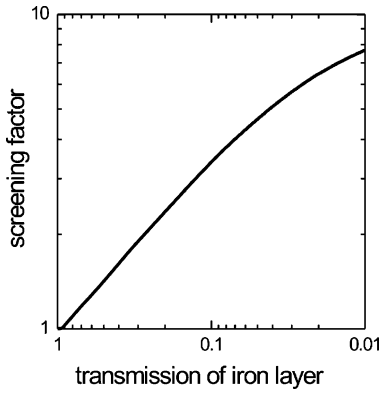

Figure 6. Calculation of the screening factor for isotropic oscillators with resonance frequency at 2062 cm^{-1} on a smooth metal film in normal transmission configuration versus the transmission of the metal film. For the calculation we assume bulk properties (Fe) for the metal film.

$$\frac{\Delta R}{R} = 1 - \frac{R_{CO/Fe/MgO}}{R_{Fe/MgO}} \approx 4\frac{\omega}{c}\cdot\frac{\sin^2\phi}{\cos\phi}\cdot n_{CO}\cdot \mathrm{Im}\alpha_{CO\perp} \qquad (5)$$

with $\alpha_{CO\perp}$ as the complex frequency dependent surface polarizability component perpendicular to the surface and n_{CO} the area density of adsorbate molecules. The approximation (5) is valid for an adsorbate layer on a thick and continuous metal film and for $|\epsilon_m|\cdot\cos^2\phi \gg 1$, which is fulfilled for the sample we consider in ref 8. In the thin film approximation the relative transmittance $\Delta T/T$ for an adsorbate layer on the dielectric substrate at normal incidence of light approximately is

$$\frac{\Delta T}{T} = 1 - \frac{T_{CO/Fe/MgO}}{T_{Fe/MgO}} = 2\frac{\omega}{c}\cdot\frac{1}{(1+n_s)}\cdot n_{CO}\cdot \mathrm{Im}\alpha_{CO\parallel} \qquad (6)$$

according to ref 37 with $\alpha_{CO\parallel}$ as the surface polarizability component parallel to the surface and n_s as the refractive index of the transparent substrate. For the hypothetical transmittance change due to a CO arrangement on the metal island walls $\alpha_{CO\parallel}$ has to be substituted by $\alpha_{CO\perp}/2$ (in transmission we use nonpolarized light; therefore half of the vibration of the CO molecules is in field direction). Doing so, from the IRAS spectra in ref 8 with $\phi = 75°$, with $n_s = 1.7$ (for MgO), and under consideration of the effective CO covered area from the above estimate, it follows $\Delta T/T$, which is 130 times smaller than the observed signal height for CO on 20 nm Fe/MgO at 2055 cm^{-1} (CO vibration on Fe(001)). That enhancement of 130 is the lower limit of the real enhancement because the screening due to the metal film lowers $\Delta T/T$ by a factor of $1/S(d)$. To demonstrate this effect of screening due to the metal film in transmittance, we performed numerical calculations with commercial software.[38] We calculated S for a simple model: The peak size in transmittance for a system consisting of a layer of model oscillators on a thick MgO substrate is divided by the peak size of the same oscillators on a smooth Fe layer on MgO. Figure 6 shows that for thicker films with low transmission, the screening S becomes significant for the size of the absorption peak. Taking into account S for the measured transmittance value, we find an enhancement of approximately 320 for the CO absorption on the 20 nm thick metal film. Due to the broader line width of the CO absorption signal on the rough films compared to the lines measured in reflectance from smooth films and due to the asymmetry of the absorption lines, we further underestimated the enhancement. Because of the screening

effect, a slightly smaller CO signal size is observed for the thickest film, despite the suggested increase in the effective CO covered area due to the columnar film growth. Because the films above 25 nm thickness do not show the strong SEIRA decrease with an increase in thickness as is known for the growth of continuous films,[29,35] they seem to stay at the percolation threshold in accordance with our findings from above.

Another way to estimate the enhancement is a line shape analyses, as described in ref 39. The asymmetry of the absorption line was fitted by a Fano-like susceptibility of the adsorbate system.[39,40] In the case of the 20 nm thick metal film we found an enhancement of about 400 in reasonably good agreement with the other estimate.

4. Conclusions

The IR spectra of CO show that on well ordered iron films strong SEIRA effect exist. The IR spectra of the metal films and the IR spectra of the adsorbed CO indicate that iron films grown at 400 °C on a UHV cleaved MgO(001) surface stay near the percolation even for thicknesses up to 32 nm. With increasing coverage the metal cuboids primarily grow in height; consequently, the metal island become increasingly steep. The frequencies of the absorption features indicate that the side faces of the islands consist of (100) facets as well as (110) facets, but the ratio between these facets changes toward (100) with increasing metal coverage. The CO exposure at which the size of the IR-absorption peak saturates is proportional to the film thickness. This is related to the fact that we measure the CO molecules in the groves of the film.

Acknowledgment. We thank A. Otto for valuable discussions. This project is supported by the Deutsche Forschungsgemeinschaft (DFG).

References and Notes

(1) Thürmer, K.; Koch, R.; Weber, M.; Rieder, K. H. *Phys. Rev. Lett.* **1995**, *75*, 1767.
(2) Mezey, L. Z.; Giber, J. *Jpn. J. Appl. Phys., Part 1* **1982**, *21*, 1569.
(3) Overbury, S. H.; Bertrand, P. A.; Samorjai, G. A. *Chem. Rev.* **1975**, *75*, 547.
(4) Brune, Harold; Bales, G. Steven; Jacobsen, Joachim; Boragno, Corrado; Kern, Klaus. *Phys. Rev. B* **1999**, *60*, 5991.
(5) Zuo, J. K.; Wendelken, J. F. *Phys. Rev. Lett.* **1997**, *78*, 2791.
(6) Vitos, L.; Ruban, A. V.; Skriver, H. L.; Kollar, J. *Surf. Sci.* **1998**, *411*, 186.
(7) Krauth, O.; Fahsold, G.; Pucci, A. *J. Chem. Phys.* **1999**, *110*, 3113.
(8) Priebe, A.; Geyer, W.; Fahsold, G.; Pucci, A. *Surf. Sci.* **2002**, *502*, 388.
(9) Lawler, J. F.; Schad, R.; Jordan, S.; van Kempen, H. J. *J. Magn. Magn. Mater.* **1997**, *165*, 224.
(10) Jordan, S. M.; Schad, R.; Keen, A. M.; Bischoff, M.; Schmool, D. S.; van Kempen, H. *Phys. Rev. B* **1999**, *59*, 7350.
(11) Jordan, S. M.; Schad, R.; Herrmann, D. J. L.; Lawler, J. F.; van Kempen, H. *Phys. Rev. B* **1998**, *58*, 13132.
(12) Fahsold, G.; Priebe, A.; Magg, N.; Pucci, A. *Thin Solid Films* **2000**, *364*, 177.
(13) Stroscio, J. A.; Pierce, D. T.; Dragoset, R. A. *Phys. Rev. Lett.* **1993**, *70*, 3615.
(14) Fahsold, G.; Priebe, A.; Pucci, A. *Appl. Phys. A* **2001**, *73*, 39.
(15) Berthier, S.; Peiro, J. *J. Phys. III Fr.* **1997**, *7*, 537.
(16) Zhang, X.; Stroud, D. *Phys. Rev. B* **1995**, *52*, 2131.
(17) Dvoynenko, M.; Goncharenko, A. V.; Romaniuk, V. R.; Venger, E. F. *Physica B* **2001**, *299*, 88.
(18) Luck, J. M. *Phys. Rev. B* **1991**, *43*, 3933.
(19) Fahsold, G.; Bartel, A.; Krauth, O.; Magg, N.; Pucci, A. *Phys. Rev. B* **2000**, *61*, 14108.
(20) Priebe, A. Ph.D. thesis, University of Heidelberg, 2002.
(21) Kim, Y. H.; Tanner, D. B. *Phys. Rev. B* **1989**, *39*, 3585.
(22) Marquardt, Peter; Nimtz, Günter. *Phys. Rev. Lett.* **1986**, *57*, 1036.
(23) Fahsold, G. Thesis of habilitation, Universität Heidelberg, 2002.
(24) Benndorf, C.; Rüger, B.; Thieme, F. *Surf. Sci.* **1985**, *163*, L675.
(25) Erley, E. *J. Vac. Sci. Technol.* **1981**, *18*, 472.
(26) DMoon, D. W.; Bernasek, S. L.; Lu, J. P.; Gland, J. L.; Dwyer, D. J. *Surf. Sci.* **1987**, *184*, 90.
(27) Fujii, J.; Galaktionov, M.; Giovanelli, L.; Panaccione, G.; Bodino, F.; Vobornik, I.; Rossi, G. *Thin Solid Films* **2003**, *428*, 30.
(28) Fahsold, G.; Sinther, M.; Priebe, A.; Diez, S.; Pucci, A. *Phys. Rev. B* **2002**, *65*, 235408.
(29) Priebe, A.; Sinther, M.; Fahsold, G.; Pucci, A. *J. Chem. Phys.* **2003**, *119*, 4887.
(30) Fahsold, G.; Sinther, M.; Priebe, A.; Diez, S.; Pucci, A. *Phys. Rev. B* **2004** *70*, 115406.
(31) Jakob, P.; Persson, B. N. J. *Phys. Rev. B* **1997**, *56*, 10644.
(32) Luck, J. M. *Phys. Rev. B* **1991**, *43*, 3933.
(33) Sinther, M.; Pucci, A.; Otto, A.; Priebe, A.; Diez, S.; Fahsold, G. *Phys. Status Solidi A* **2001**, *188*, 1471.
(34) Otto, A. *Phys. Status Solidi A* **2001**, *188*, 1455.
(35) Krauth, O.; Fahsold, G.; Magg, N.; Pucci, A. J. *J. Chem. Phys.* **2000**, *110*, 3113.
(36) Langreth, D. C. *Phys. Rev. B* **1989**, *39*, 10020.
(37) Lehmann, A. *Phys. Status Solidi B* **1988**, *148*, 401.
(38) SCOUT (software package for optical spectroscopy), supplied by Soft Science, Aachen, Germany.
(39) Priebe, A.; Fahsold, G.; Pucci, A. *Surf. Sci.* **2001**, *482*, 90.
(40) Langreth, D. C. *Phys. Rev. B* **1985**, *54*, 126.